THE ASTROPHYSICAL JOURNAL, 272:563–578, 1983 September 15

A FAR-ULTRAVIOLET EXTINCTION LAW: WHAT DOES IT MEAN?

J. MAYO GREENBERG AND GRZEGORZ CHLEWICKI[1]
Laboratory Astrophysics, University of Leiden, Leiden, The Netherlands
Received 1982 September 24; accepted 1983 March 8

ABSTRACT

The dust grains in the diffuse cloud medium are characterized by a far-ultraviolet (FUV) extinction "law" so that all curves have the same functional form for inverse wavelengths $\lambda^{-1} \gtrsim 6$ μm^{-1}. A direct theoretical consequence of this fact is that there is very little scattering (essentially pure absorption) by either the particles responsible for the FUV extinction or the 2200 Å hump. A strong correlation between the strength of the 2200 Å hump and the visual extinction is confirmed. Poor correlation is found between the FUV extinction and either the 2200 Å hump or the visual extinction. All indications are that the dust grains responsible for the visual, the 2200 Å hump, and the FUV extinction are a trimodal distribution of independent groups of particles of which the latter two are rather strictly limited in radii (if treated as spheres) to $a \lesssim 0.01$ μm. It is shown that graphite particles of this size which can produce the strength of the 2200 Å hump can make at most an insignificant contribution to the FUV extinction. This leads to the fact that even very small quantities of graphite grains of sizes > 0.01 μm must be excluded even if they appear to be required to produce the desired hump shape. This criterion is applied to several grain models. It is further shown, subject to the above criterion, that no Mie theory calculations using currently accepted graphite or silicate optical properties can provide the observed shapes of the ultraviolet and FUV extinction. Implications of the correlations and noncorrelations of the several components of the full extinction curve are used to derive some characteristics of the physical evolution of grains outside of molecular clouds.

Subject headings: interstellar: grains — interstellar: matter — ultraviolet: spectra

I. INTRODUCTION

As soon as it became possible to make observations of interstellar extinction from above the Earth's atmosphere, it was evident that the apparent saturation at about $\lambda^{-1} = 4$ μm^{-1} which had been suggested by ground-based measurements was misleading. The earliest rocket observations (Boggess and Borgman 1964; Stecher 1965) already showed a continued rise in the extinction in the ultraviolet. Furthermore a new structure—now identified as the 2200 Å (4.6 μm^{-1}) hump—was indicated (Stecher 1965). Satellite observations with *OAO 2* (Bless and Savage 1970, 1972) not only confirmed and clarified the structure at about 4.6 μm^{-1} but showed that following the subsequent dip in extinction at about 5.8–6.2 μm^{-1} there was again a rise in the extinction as far as the instrument could detect.

Since it is not the purpose of this paper to review all the ultraviolet extinction observations, we shall now summarize briefly the current status of knowledge of the extinction beyond $\lambda^{-1} \approx 4$ μm^{-1} as a background to our own contribution.

It was natural to attempt to derive correlations between the visual extinction, the 2200 Å hump, and the far-ultraviolet (FUV) extinction. Indeed, it has been found that, excluding such notable exceptions as θ^1 Orionis and the Scorpio-Ophiuchus stars, there is an excellent correlation between the hump and the visual extinction (Savage 1975; Nandy *et al.* 1975; Dorschner, Friedeman, and Gürtler 1977). However, attempts at correlating the hump with the FUV extinction have not been successful although such cases as θ^1 Orionis and the less extreme Scorpio-Ophiuchus stars seem to show that when the hump is reduced, the FUV extinction curve is flatter. Savage (1975) noted this to occur in H II regions where also the visual extinction is modified in the sense of having a generally higher value of the total to selective extinction. Other cases of variability of the ultraviolet portion of the extinction curve are Herbig shell stars (Sitko, Savage, and Meade 1981).

In spite of the lack of correlation between all three portions of the extinction curve it was nevertheless considered useful for practical purposes to derive an average curve over the full spectral range. Although this has often been recognized as inconsistent, it has been customary to assume, as was done by Bless and Savage, that the lack of correlation of the 2200 Å hump and the FUV extinction results from the differences between a variety of special objects rather than differences in a

[1]On leave of absence from N. Copernicus University, Torun, Poland.

single defined region. It is interesting that in a study of the relationship between the 4430 Å diffuse band and the hump expressed as a color excess, $E(22-V) = A(2160\ \text{Å}) - A(V)$, it was noted (Wu, York, and Snow 1981) that while the 4430 band intercorrelates with $E(22-V)$ and $E(B-V)$, it is not well correlated with $E(18-V)$. This could only be a hint about the FUV because, unfortunately, the *ANS* data which they used does not extend far enough beyond the dip at ~1500 Å to probe the FUV component reliably.

In general the observational samples from which correlations have been extracted span a variety of physically different regions so that one expects that all three extinction components may be individually subject to variability via growth, destruction, radiation pressure, etc. We have tried to avoid such complications by limiting ourselves to a sample in which at least the visual portion of the extinction curve may be presumed to be uniform; i.e. the diffuse interstellar medium. Thus we avoid obvious dense clouds along the line of sight and even try to eliminate stars which may have very recently emerged from a region of new star formation and which may still have significant local interstellar material associated with such objects. Since we shall be dealing only with young stars, it is difficult to fully eliminate local extinction contributions. However, in all our cases we require that the line-of-sight contribution far exceeds that of any local material.

Whereas, in the past, tradition has led to normalization of all extinction curves based on the visual, i.e., $E(\lambda-V)/E(B-V)$, we shall try to avoid prejudging correlations by normalizing separately in the three major areas. The suggestion for this is illustrated in Figure 1 where a mean extinction curve is schematically divided into three components (Greenberg 1973, 1978). We note that the particles responsible for the visual extinction are too large to produce the FUV extinction because their mean size of ~ 0.1 μm is such as to have scattering properties which produce a saturation at wavelengths shortward of about $\lambda^{-1} \approx 4\ \mu\text{m}^{-1}$ independent of their material optical properties (see van de Hulst 1957; Greenberg and Shah 1969; Greenberg 1978). Consequently color excesses $E(\lambda - V)$ where λ is in the ultraviolet combine portions of the extinction which may be contributed by different populations of particles. It is interesting to note here that Massa (1980), using a quite general method of analyzing the ultraviolet extinction but still using the standard excess $E(\lambda - V)$, concludes that the 2200 Å hump and the FUV extinction require separate particles as was postulated as a possibility in deriving Figure 1. Since Massa used relatively nearby ordinary B dwarfs in his sample, he should have had little if any contributions from local dense material; i.e., his sample was like ours in that he explored what we call the general diffuse cloud medium. We have used young stars and have therefore probed far deeper—up to about 3 kpc—into the diffuse medium.

Our normalization procedure is suggested by the separate particle concept indicated by components labeled (3) and (4) in Figure 1, where these extra contributions are taken relative to a saturation level schematically extrapolated beyond $\lambda^{-1} = 4\ \mu\text{m}^{-1}$. This procedure should have no *a priori* influence on the final results except to make it easier to focus attention on the shapes in the separate spectral regions of the extinction curve and to clarify the degree of correlation between them. As justified in detail in § III, we normalize the hump region between 2500 Å and 2160 Å and the FUV region between 1700 Å and 1300 Å. The apparent fact that, regardless of the amount of extra extinction in this latter region, all curves (relatively flat or otherwise) appear to continue to bend upward at sufficiently short wavelengths, led to the conjecture that there may be a uniform curvature in the FUV extinction (Greenberg and Hong 1974). This was one of the prime motivations for pursuing the problem as we have, although we have

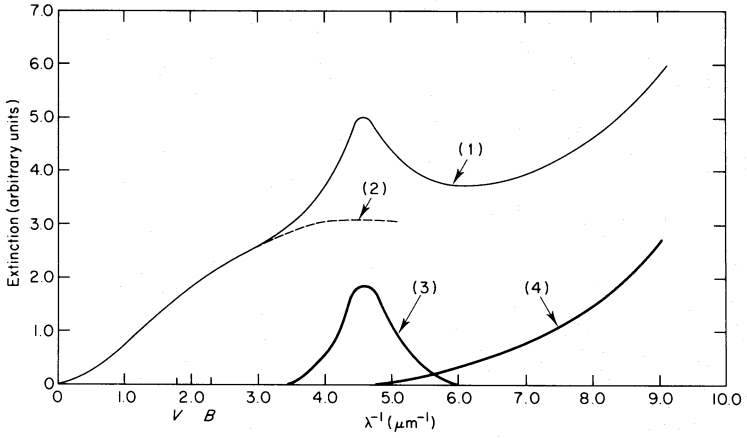

FIG. 1.—Schematic representation of the mean extinction curve (1). The "visual" portion (2) is the contribution made by classical size particles (radius ~ 0.1 μm). The hump (3) and the far-ultraviolet portion (4) are produced by much smaller particles.

not included the kinds of variabilities seen in regions of new star formation or in molecular clouds. We shall see that in the general diffuse cloud medium there is indeed a strong suggestion of a uniform FUV extinction curve which has some important theoretical consequences in defining criteria for grain models.

II. REDUCTION OF DATA

The research program discussed here was based on spectra obtained by the *IUE* satellite and subsequently made available to all astronomers through the *IUE* data bank. Ultraviolet spectrographs on board the *IUE* cover the spectral range from ~1150 Å to ~3200 Å and provide two spectral resolutions: the so-called high and low dispersions corresponding, respectively, to spectral resolving powers of ~0.2 Å and ~7 Å (Boggess *et al.* 1978*a*, *b*). The wavelength range covered by the telescope has been divided into two partly overlapping sections, 1150–2000 Å and 1800–3200 Å, which are observed with two separate spectrographs.

Within the total range of stellar brightness observable by the *IUE*, there is only a relatively narrow interval of a few visual magnitudes where both low- and high-resolution images can be obtained. Brighter stars can usually be observed only in high dispersion, whereas faint stars, approaching the limiting magnitude of the telescope, can only be reached with low-dispersion exposures. Since one of the aims of our research was to establish the degree of correlation between interstellar extinction in different spectral regions, it was necessary to cover the widest possible range in $E(B-V)$ for every spectrum/luminosity class. Low-reddened stars tend to be brighter, whereas among more heavily obscured objects we often find very faint distant stars. Therefore, it was necessary to work with both high- and low-dispersion images even though it complicated the reduction of the data and lowered the accuracy of some of its results.

The data reduction procedure had to be aimed at converting both low- and high-dispersion spectra into a similar form, and simultaneously reducing the noise level, which for fainter objects becomes unacceptably high. Since we were interested in the analysis of large-scale features in the continuum of reddened stars, we decided to use spectra converted to a relatively low resolution of about 35 Å. The final values of flux for each object were calculated on a uniform grid of points with 10 Å stepping as a convolution with a Gaussian function, the half-width of which was regarded as the effective resolution. Data obtained with the use of this method could be compared easily with TD-1 satellite spectra (Jamar *et al.* 1976; Macau-Hercot *et al.* 1978). This procedure turned out to be extremely important for the evaluation of the quality and reliability of *IUE* material and for the estimation of errors.

The factor which determined the scope of our research and severely limited the number of stars used in the study was the quality of *IUE* spectra. We shall discuss here those of the shortcomings of *IUE* observations which proved to be important for our work.

The photometric calibration of low-dispersion spectra is known with an accuracy of about 10%, which leads to possible deviations as high as ~0.1 mag (Bohlin *et al.* 1980). One has to remember that because long and short wavelength spectra are calibrated separately, the 0.1 mag error is inherent in any procedure used to link up two images of a single object. This fact may mean some amplification of calibration errors within one of the two spectral ranges.

The sensitivity of both spectrographs is a function of wavelength, and so is the accuracy with which the calibration function is known. In particular, the sensitivity falls rapidly towards the short wavelength boundary of both spectral ranges. This decline of sensitivity most affects spectra with a prominent 2200 hump. The sensitivity at 2200 Å is already 5 times lower than at 2800 Å (where it reaches a maximum), and the decline becomes very steep for $\lambda < 2100$ Å. Because of this the 2200 hump region in heavily reddened spectra is usually underexposed causing uncertainties in its peak region and the short wavelength wing. Consequently, evidence of possible differences in the shape of the hump ($1850 < \lambda < 2400$) coming from *IUE* data must be viewed with caution.

The dynamical range of sensitivity is rather low for the *IUE*, with software saturation occurring at 10 times the average instrumental background level. For low-dispersion spectra it is possible to expose two images during one working cycle of the camera, thus allowing the observer to widen the energy range of the spectrograph. Using, on the one hand, numbers given by various *IUE* observers and, on the other hand, examining the spectra from our sample, we arrived at the same estimate of the maximum reddening which can be reached with the *IUE*. For early-type stars with normal strength of the 2200 hump (see § III), $E(B-V) = 1.0$ to 1.1 mag seems to be the maximum value for which a spectrum can be properly exposed throughout the *IUE* region. However, with only a single exposure within the long wavelength range, serious difficulties already appear at $E(B-V) = 0.3$ to 0.4. mag.

Absolute calibration of *IUE* spectra requires precise knowledge of exposure times, which for spectra in the data bank are sometimes uncertain. One of the consequences is that the procedure used to link the long and short wavelength spectrum of the same object has to be based on the comparison of average energy levels in the region where the spectra overlap. For some spectra, such comparison proves difficult because of very low signal-to-noise ratio in the long wavelength image for 1800 Å $< \lambda <$ 2000 Å. This fact forced us to reject some of the more strongly reddened stars from our initial sample.

High-dispersion spectra pose even more difficult problems than those which have already been discussed for low-resolution images. Not only is one additional step necessary in the reduction procedure (the transformation of an echelle-grating spectrum into a sequential set of data), but also the long wavelength spectrum is always limited to a single exposure and a smooth linkage with the short wavelength image already becomes difficult for $E(B-V)=0.3$ to 0.4 mag. The overall accuracy of calibration is also much lower for high-resolution data, especially in the short wavelength regions of both spectral ranges. The linking procedure provides a check on calibration errors at the boundary of the long wavelength range. However, for $\lambda \geq 1500$ Å, such errors are difficult to detect and can easily reach 1 mag. The only way to detect calibration errors in that region is to compare *IUE* high-dispersion data with low-dispersion images or with spectra obtained with other instruments. *TD-1* observations proved particularly useful, because of the relatively large number of stars observed with that instrument. Calibration errors severely reduced our sample of reliable spectra, because we decided to reject not only those with larger errors but also all high-dispersion images for which confirmation of photometric accuracy was impossible. Four standard stars observed in high dispersion were only slightly affected by inaccurate calibration, their errors being ~ 0.2 mag at 1380 Å, and a simple corrective function was derived to improve the calibration. The discrepancies still remaining between comparison spectra and high-dispersion images included in our final sample (Table 1) are smaller than 0.1 mag.

Spectra of early-type stars are characterized by numerous strong and broad lines originating in massive stellar winds. Such features can vary significantly even within a single spectral sub-class (Henize, Wray, and Parsons 1982) and thus they can seriously influence the characteristics of extinction derived from those spectra. In order to remove or suppress such strong spectral lines, we used an algorithm based on a somewhat modified median filter together with a set of other simple numerical filters. For most of the stars in our sample, the effectiveness of our smoothing procedure was at least as good as that illustrated in Figure 2 for the rather extreme O star HD 242908. There were however a few

TABLE 1

BASIC EXTINCTION PARAMETERS FOR A SAMPLE OF EARLY-TYPE STARS

HD/BD	*IUE* Image[a]	Sp/L	$E(B-V)$	$E(22-25)$[b]	$E(13-17)$[b]	2200 A[c]	FUV[c]	Remarks
66811 ...	3066,3487 (H)	O5 f	0.06	...	...	...	...	Standard
47839 ...	2471,2777 (L)	O7 V	0.07	...	...	...	...	Standard
164794 ...	5257,6071 (L)	O4 V	0.35	0.87	0.25	+	(+)	
303308 ...	2356,2650 (L)	O3 V	0.45	1.04	0.50	+	(+)	
46150 ...	5885,6925 (L)	O5 V	0.45	1.25	0.35	+	(+)	
46223 ...	2421,2714 (H)	O4 V	0.54	1.51	0.87	+	+	
206267 ...	4649,5388 (H)	O6.5 V	0.54	...	1.21	...	+	
242908 ...	7270,8341 (L)	O4 V	0.60	1.67	0.71	+	+	
15629 ...	7273,8287 (L)	O5 V	0.74	...	0.96	...	+	
14947 ...	7220,8284 (L)	O5 If	0.77	...	1.54	...	+	
+60°497 ...	3660,4155 (L)	O6 V	0.77	...	1.88	...	+	
+60°501 ...	3645,4114 (L)	O7 V	0.77	2.15	1.19	+	+	
+60°507 ...	3641,4111 (L)	O5 f	0.77	...	1.01	...	+	
+60°513 ...	3661,4131 (L)	O7 V	0.81	2.12	1.49	+	+	
15558 ...	7222,8286 (L)	O5 III	0.85	2.13	1.02	+	+	
+60°501 ...	3644,4113 (L)	O6	0.86	2.22	1.07	+	+	
15570 ...	3643,4112 (L)	O4 If	1.02	2.69	1.72	+	+	
52089 ...	3147,3573 (H)	B2 II	0.0	...	...	...	...	Standard
53138 ...	7102,8168 (L)	B3 Ia	0.03	...	...	...	...	Standard
42087 ...	2527,2839 (H)	B2.5 Ib	0.38	1.18	1.02	+	+	
14818 ...	8161,9416 (H)	B2 II	0.48	...	0.95	...	+	
206165 ...	3939,4406 (H)	B2 Ib	0.48	1.33	1.26	+	+	
41117 ...	3021,3436 (H)	B2 IA	0.51	1.57	0.94	+	+	
198478 ...	7301,8563 (L)	B3 Ia	0.54	...	0.61	...	+	
148379 ...	2502,2808 (L)	B2 Ia	0.80	2.10	...	(+)	...	
42690 ...	5572,6488 (L)	B2 V	0.01	...	...	...	...	Standard
147889 ...	2410,2699 (L)	B2 V	1.10	2.30	1.40	...	...	

[a] The first and second numbers refer to the long and short wavelength spectra respectively; letters "H" and "L" indicate the original dispersion.

[b] Color excesses $E(22-25)$ and $E(13-17)$ for O stars have been corrected for the effects of nonzero reddening of the standard stars.

[c] Stars marked with "+" were used in the derivation of the average extinction curve as well as the correlation with $E(B-V)$. Stars marked with "(+)" were only used in calculating the correlations with $E(B-V)$. All standard stars were used in both the 2200 A region and the far-ultraviolet.

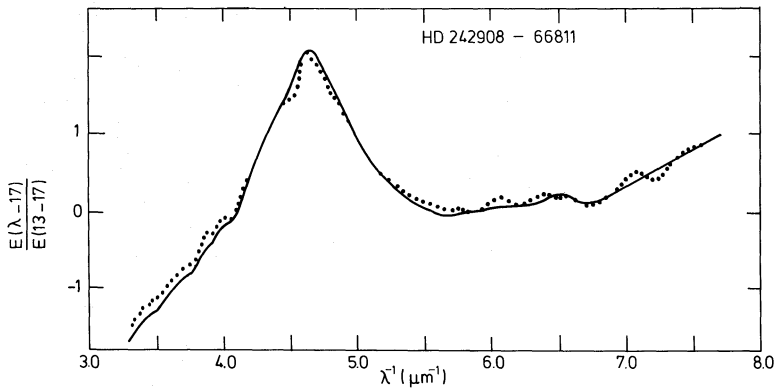

FIG. 2.—Effectiveness of the smoothing algorithm. The solid line is the extinction curve for HD 242908 after smoothing. The standard star is HD 66811. The dots are the same extinction curve derived from unsmoothed spectra. Both curves are normalized between 5.88 μm^{-1} and 7.70 μm^{-1}. The apparent shift between the two curves for $\lambda^{-1} < 4.0$ μm^{-1} is an artifact produced by the small difference between the values of the FUV color index for smoothed and unsmoothed spectra.

exceptions among extremely early-type stars with mass-loss characteristics intermediate between Of and WN stars (e.g., HDE 303308; Walborn 1982 and references therein). The filtering was always carried out on spectra with an effective resolution of ~ 7 Å so that high-dispersion images first had to be reduced to that form by convolution with a Gaussian function of appropriate width.

A summary of the data reduction procedure is as follows: 1. Calibration, construction of a single image covering the whole *IUE* region. 2. Reduction of the effective resolution to 7 Å (for high-dispersion spectra only). 3. Removal of lines by numerical filters. 4. Reduction of the effective resolution to 35 Å, derivation of extinction curves.

It has already been mentioned that instrumental effects caused a very severe reduction of the number of stars in our sample. We began our study with 70 objects and, after the reduction procedures had been carried out, only 27 objects with reliable continuum characteristics remained. Because of uncertain calibration it is impossible to reduce instrumental errors below 0.1 mag. Furthermore, because no reliable prediction of the UV spectrum can be made for early-type stars with strong stellar winds, there may be differences between the intrinsic energy distributions of the reddened and corresponding standard stars. Direct comparison between otherwise similar stars with different stellar winds indicates that the errors introduced by assuming identical UV spectra are comparable with the *IUE* photometric error of ~ 0.1 mag. This is consistent with the upper limit implied by the results of Holm and Cassinelli (1977). Errors of this kind are not expected to affect the curvature of the FUV extinction. On the other hand, the absolute values of the color excess $E(13-17)$ may be off by as much as 0.2 mag in exceptional cases. Finally, we have to emphasize that no numerical quality criterion can be used to separate beyond doubt "good" and "bad" *IUE* spectra. In a few cases, different criteria produced contradictory results, and the final decision to include certain objects in our sample reduced itself to a matter of judgement. For example, all results for the short wavelength spectra of BD +60°497, BD +60°507, and possibly BD +60°513 and HD 15570, to which this remark applies, should be treated with caution. Nevertheless, for most of the stars in Table 1 the total error is determined only by the *IUE* photometric accuracy of 0.1 to 0.15 mag. For a few objects the two other possible sources of error may bring this figure up to 0.2 or 0.3. mag. Therefore we rejected from our sample all stars for which the magnitude of extinction effects was comparable with that number, which in practical terms meant that stars with $E(B-V)$ less than ~ 0.3 mag could not be accepted.

The stars listed in Table 1 provide a farily complete coverage in reddening for early O types. A few B stars in the sample enabled us to confirm that extinction characteristics obtained here did not depend on spectral type and could be treated as genuine interstellar physical features.

III. RESULTS

a) *The Far-Ultraviolet Extinction*

The data which was smoothed as described in § II has been averaged for 17 stars and normalized to a color excess of $E(1300\ \text{Å}-1700\ \text{Å})=1$ [hereafter referred to as $E(13-17)$] and $A(1700\ \text{Å})=0$. The 1700 Å point was chosen for the long wavelength end because we anticipated that the contribution by the material responsible for the hump would be smallest at or near the minimum in the extinction curve. This happens also to coincide with a region which is relatively free of circumstellar lines. In Figure 3 a comparison is made between the average FUV extinction and the individually normalized

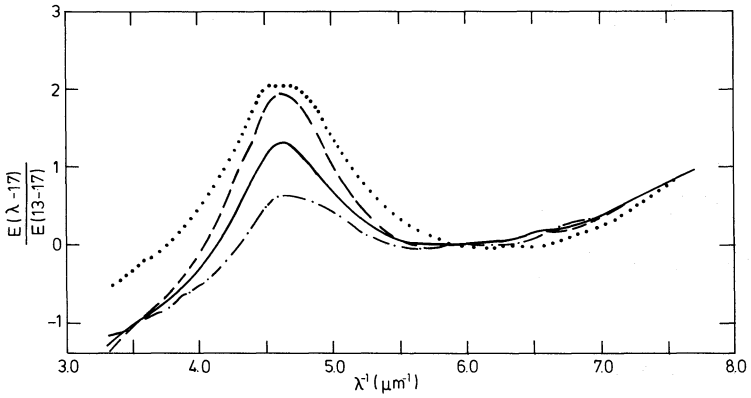

FIG. 3.—Far-ultraviolet extinction curves: the average for 17 stars (*solid*); BD +60°502 (*dashed*); HD 42087 (*dash dot*); peculiar star HD 147889 (*dots*). All curves are normalized at $\lambda_1 = 1700$ Å (5.88 μm^{-1}) and $\lambda_2 = 1300$ Å (7.7 μm^{-1}). Some of the spectra used to derive the average FUV extinction curve were of poor quality in the 2200 hump region (see text). The average curve is relatively unreliable in determining the shape and position of the hump.

extinction curve for three stars: BD +60°502, HD 42087, and HD 147889. The first two stars were chosen as representative of the variations in the sample of 17 stars with normal visual extinction which we used in the average. The third, HD 147889, was chosen as a highly exceptional case, not representative of the diffuse medium since $R = A(V)/E(B-V)$ is significantly greater than the average value of 3.1 (Whittet, van Breda, and Glass 1976; Whittet and van Breda 1975).

The first important characteristic we want to point out is the exceptional degree of uniformity in the *shape* of the extinction curve in the range 1700 Å $\leq \lambda \leq$ 1300 Å. This uniformity is impressively supported by the result that the standard deviation (S.D.) for the 17 star sample is only S.D. $\approx$ 0.07 mag which is smaller than the error level. It should be noted that even without smoothing, the standard deviation is only slightly raised, being S.D. $\leq$ 0.09 mag. The uniformity of the FUV extinction appears to be substantially higher than even that for the visible for which it is customary to assume a kind of "law" to be used for stellar calibrations and distances. No questions can arise here of linking the short and long wavelength *IUE* spectra because we have normalized between two points which lie exclusively in the former range.

Although the FUV extinction exhibits such a uniform curvature for all the stars in the sample its magnitude is certainly not correlated with the amount of visual extinction. The variability of the ratio of $E(13-17)$ to $E(B-V)$ is shown in Table 1. For example, the star BD +60°502 has $E(13-17) = 1.073$ and $E(13-17)/E(B-V) = 1.25$, while HD 42087 has $E(13-17) = 1.020$ and $E(13-17)/E(B-V) = 2.28$. As one can see in Figure 3, even though these stars differ in their relative amounts of FUV extinction by a factor of 2, there is no distinguishable difference in their curvature. This is an indication of a uniformity in the type of particle responsible for the FUV extinction as will be discussed in § V. On the other hand, the uniformity in the FUV extinction certainly does not extend into the 2200 Å hump region. Even though BD +60°502 and HD 42087 look the same in the FUV, there is a substantial difference in the relative strength of their humps.

Finally we note an apparent tendency for the majority of extinction curves to have a negative curvature between 3.5 and 4 μm^{-1}, indicating that saturation of the visual extinction is beginning to set in just before the onset of the 2200 Å absorption feature.

b) *The 2200 Å Hump*

We chose to normalize the strength of the hump between 2500 Å and its mean maximum at 2160 Å. The former was chosen for two reasons: (1) The turnover point in the visual–near-UV extinction occurs at approximately 3.5 μm^{-1} indicating "saturation" at *about* 4 μm^{-1} so that by choosing 2500 Å as the long wavelength end we hope to avoid mixing a "visual contribution" with that of the hump; and (2) 2500 Å lies outside the 2600 Å region which contains Fe and Mg lines.

In Figure 4 the average of the ultraviolet extinction curves for the 13 star sample used for the hump is presented in normalized form with $E(22-25) = 1$ and $A(25) = 0$. The relatively poor quality of the data in this spectral region does not allow us to say any more about the shape of the hump other than what has already been stated elsewhere, namely, that the shapes all look *pretty much* the same (Savage 1975; Bless and Savage 1972; Nandy *et al.* 1975; Seaton 1979). In the range $3.5 \geq \lambda^{-1} \geq 5.5$ μm^{-1} the standard deviation is S.D. $\approx$ 0.2 mag, and there is an instrumentally produced sudden increase from < 0.1 to 0.15 just in the connecting spectral region at about 5.2 μm^{-1}. The same comparison stars are shown in Figures 4 and 3. The two stars within the

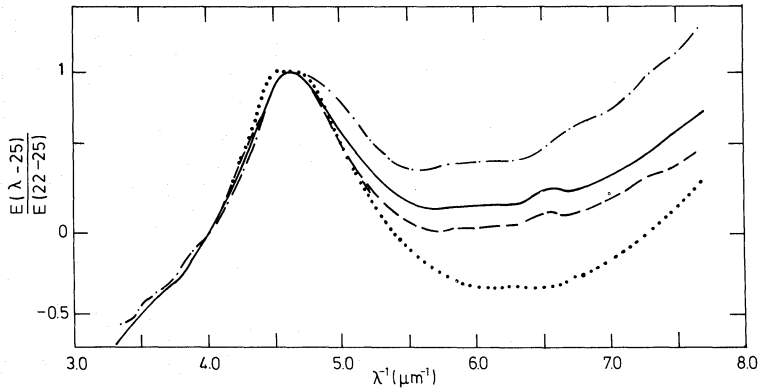

FIG. 4.—The 2200 Å hump. The normalization points are: $\lambda_1 = 2500$ Å (4.0 μm^{-1}) and $\lambda_2 = 2160$ Å (4.63 μm^{-1}, the peak wavelength of the hump). The average for 13 stars (solid); BD +60°502 (*dashed*); HD 42087 (*dash dot*); and HD 147889 (*dots*). The apparently peculiar shape of the short wavelength wing of the 2200 hump for HD 42087 is caused by a slight underexposure in the long wavelength spectrum. This can affect the absolute level of the FUV portion beyond $\lambda^{-1} = 5.2$ μm^{-1} but without affecting its shape.

sample (HD 147889 is outside) show, as expected, substantial differences in the FUV portions and since, as we shall see, the 2200 Å hump and the visual extinction are well correlated, these differences are similar to those which are seen in curves normalized in the more customary way to $E(B-V)$. Again HD 147889, which is highly anomalous with respect to the sample, exhibits significant basic differences from the average as well as from the individual stars. We note in particular that the minimum in the ultraviolet extinction occurs at about 6.2 μm^{-1} which is shortward of that of both the average and the two stars shown. Although the minimum is too shallow to be precisely defined, this difference is large enough to be significant, since the deviations of the minimum among the sample stars are all within about 0.1 μm^{-1} of the normalization point at $\lambda^{-1} = 5.8$ μm^{-1} ($\lambda = 1700$ Å). This is not too surprising in light of the fact that HD 147889 is within the Ophiuchus cloud region and is notable for many so-called anomalous effects which make it unsuitable for inclusion in a sample which is to be representative of the diffuse cloud medium.

c) *Correlations*

We here consider correlations between the three principal spectral regions: visual, hump, and FUV, characterized respectively by $E(B-V)$, $E(22-25)$ and $E(13-17)$.

In Figure 5 the color excess $E(22-25)$ is plotted versus $E(B-V)$. It is apparent that we have not only confirmed the often stated correlation between these colors [actually, other workers use $E(22-V)$ rather than $E(22-25)$], but we also have shown that there is no significant difference between O and B stars based on our admittedly small sample. The correlation coefficient (again ignoring the exceptional case HD 147889) has an exceedingly high value of $r = 0.946$ which was calculated not including observational errors, these being difficult to evaluate. On the other hand, plotting $E(13-17)$ versus $E(B-V)$ produces the scatter diagram shown in Figure 6. A straight line drawn through these points would appear to have an intercept at positive values of $E(B-V)$, although we do not attach much significance to this. The correlation coefficient is $r = 0.656$ which is quite low and indicates that even in the average diffuse medium the visual and FUV extinction are poorly correlated.

For completeness we have plotted, in Figure 7, $E(13-17)$ versus $E(22-25)$. Here we were limited to 13 of the 14 stars in the 2200 Å hump sample, again

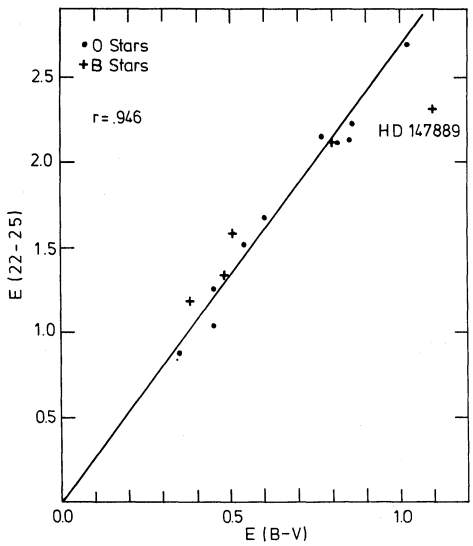

FIG. 5.—Correlation between the 2200 Å feature and the visual reddening; the correlation coefficient is r. The star which does not follow the linear relationship between the two color indices is marked separately (HD 147889).

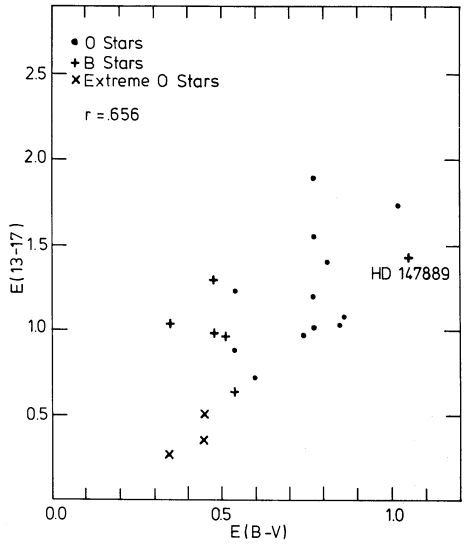

FIG. 6.—The correlation between the FUV extinction and the visual reddening. Extreme O stars (denoted by ×) were not used to calculate the average curve shown in Fig. 3 because the smoothing algorithm failed to remove strong gaseous lines from their spectra. The values of $E(13-17)$ do not seem to be significantly affected by the presence of these lines.

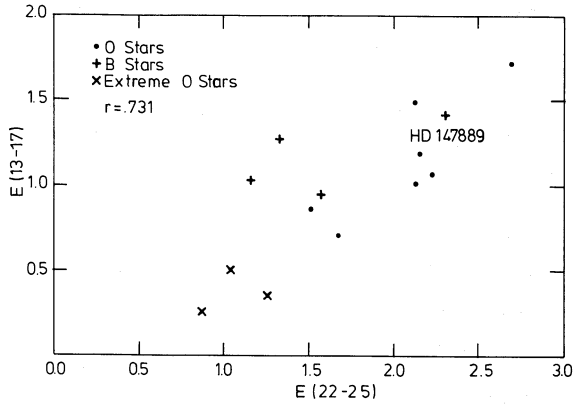

FIG. 7.—Correlation between the FUV extinction and the 2200 Å hump.

because of the poor reliability in this region. As could be anticipated from combining Figures 5 and 6, the correlation between the FUV with the hump is poor, with $r = 0.731$.

IV. OPTICAL MODELING

The lack of correlation between the FUV extinction and the hump implies that the particles responsible for each contribution must be different. As a start we have adopted the convention that graphite grains produce the hump. This is not a universally accepted idea (Duley 1976; Duley and Millar 1979; Duley, Millar, and Williams 1979; MacLean, Duley, and Millar 1982) but is certainly one for which calculations are readily performed and which can provide a basis for comparison with observations. The initial choice of material for the grains providing the FUV is some sort of silicate. We shall discover that the observations are not consistent with either of these candidates and that some significant changes in our understanding of the optical properties of these particles are required.

a) *Graphite*

Calculations of extinction by spherical graphite particles using the optical constants of Taft and Phillips (1965) and Tosatti and Bassani (1970) are presented in Figure 8. The peak values of the hump have been drawn to the same level. The sizes selected for presentation span the range of possibilities from 0.005 μm to 0.05 μm. All particles of size smaller than or equal to 0.005 μm look the same, while particles as large as 0.1 μm make such large contributions in the FUV as to be entirely inconsistent with the data if they are present in significant numbers. We have not considered the effects of nonsphericity because, although this alters the shape and position of the absorption feature, it should not greatly alter the relative contributions of this feature and the FUV which we shall ultimately use as our basic criterion of validity.

b) *Silicates*

The composition of the particles responsible for the 9.7 μm absorption associated with interstellar grains is not precisely known. Although, the prevailing idea that it is some rather undefined amorphous silicate seems well justified, this does not give us a firm basis for describing its optical properties in the ultraviolet. As a silicate it will have the general characteristics of dielectric materials all of which absorb by electronic transitions beyond some threshold photon energy. We have selected, more as illustrative examples than as definitive cases, a series of wavelength dependent complex indices of refraction starting with those obtained by Huffman and Stapp (1971, hereafter HS) for enstatite. In Figure 9*a* we present the extinction results for spherical particles of this type (denoted by Si I) normalized between 1700 Å and 1300 Å. In Figures 9*b*–9*d* the unnormalized extinction efficiencies are compared with the absorption efficiencies. This is done to show how much contribution the scattering (extinction minus absorption) makes to the extinction. We see that for particles as small as 0.005 μm the scattering is totally masked by the absorption. This is to be expected for particles whose size parameter $x = 2\pi a/\lambda$ is sufficiently smaller than unity over the wavelength range shown.

The only other available measures of the ultraviolet optical properties of silicates are those obtained by Egan and Hilgeman (1974, 1975, hereafter together EH). Their

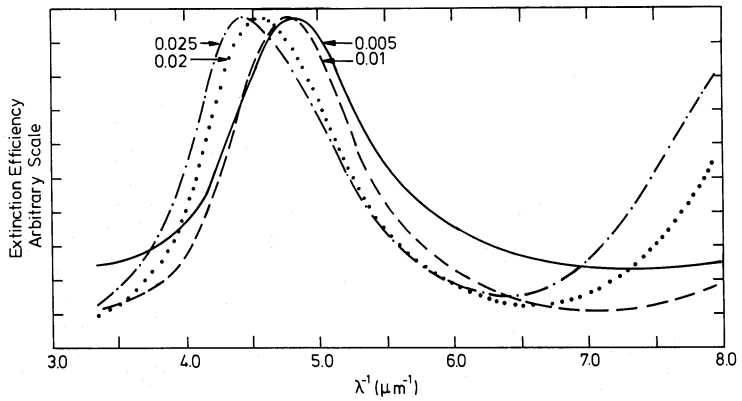

FIG. 8.—Extinction efficiencies of spherical graphite particles of radii 0.005 to 0.02 μm. All 2200 hump peaks have been drawn to the same level in order to compare the relative contribution made by each particle in the FUV.

values are very different from those of Huffman and Stapp in that the onset of absorption appears at significantly shorter wavelengths for the same sorts of silicates. It is probable that the Egan-Hilgeman results are more reliable because in their method of measurement they have avoided the effects of internal scattering in the sample which tends to amplify the effective absorptivity. Unfortunately EH have not carried their measurements out to sufficiently short wavelengths, so that there is no reliable data on possible candidate silicates as far as needed. We have somewhat arbitrarily created hypothetical materials for which the absorption first appears at the wavelength indicated by EH and which then increases with decreasing wavelength parallel to the absorptivity obtained by HS with either full or half strength, denoted respectively by Si II and Si III. Since there is no significant difference between the extinction efficiencies for these two materials except in the extinction per unit volume, we have chosen to present the results for Si III alone. In Figure 10*a* we show the normalized extinction efficiencies for this hypothetical silicate and in Figures 10*b*–10*d*, the unnormalized extinction and absorption efficiencies. The normalized efficiencies are compared with the average of the FUV extinction. It is seen in Figures 10*b*–10*d* that for particles of size $a \approx 0.005$ μm the scattering cross section may be neglected up to $\lambda^{-1} = 7.7$ μm^{-1}.

V. DISCUSSION

a) *Constraints on Grain Optics*

It is obvious from a comparison between the calculated graphite and silicate extinction curves that: (1) No single size graphite particle fits the 2160 Å hump; and (2) No single size silicate particle fits the FUV extinction. Although it is well known that by appropriate choices of size distributions and combinations of these particles one can achieve an excellent match to the *average* or any individual extinction curve, it is necessary that the observed variations can be reproduced by physically derived variations in the particles. Therefore, before attempting any detailed comparisons between the model calculations and the observations, it will prove valuable to first derive some general constraints on the grain scattering properties which are already demanded by the *qualitative* character of the observations and their deviations from an average independent of specific grain modeling.

Let us examine the implications of the uniformity of curvature in the far ultraviolet *independent* of the amount of extinction. Observational reliability permits as much as but no more than 10% deviation from this condition. Imagine that we start with some size distribution of particles which match a particular observed FUV extinction curve. To go from this extinction curve to another we must change the size distribution in some way. However, if different particles in the distribution have different wavelength dependences of extinction, the only change we can introduce consistent with the uniform curvature is a constant multiplicative factor in each population and size range. This is an unreasonable condition because it requires that whatever physical processes have led to the difference must act independently of both particle size and composition. We are thus forced to conclude that all (or at least most) of the particles which provide the FUV extinction have the same dependence of extinction cross section on wavelength *independent of size*. This can be expressed mathematically as a condition that the extinction cross section, which is generally a function of both size and wavelength, be expressable as a product of two independent functions: $C_{\rm ext}(a,\lambda) = F(a) \times G(\lambda)$. It is shown in the Appendix that such a separation of $C_{\rm ext}$ is a direct mathematical consequence of the uniform shape of the FUV extinction. The separation of the size and wavelength dependence of $C_{\rm ext}$ is achieved when the particles are such that their extinction is given fully by their

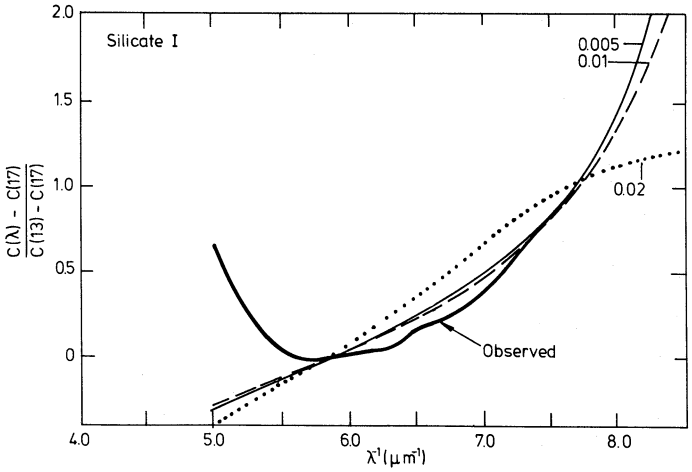

FIG. 9*a*

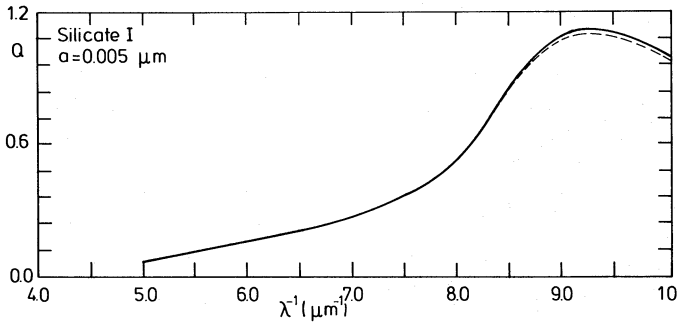

FIG. 9*b*

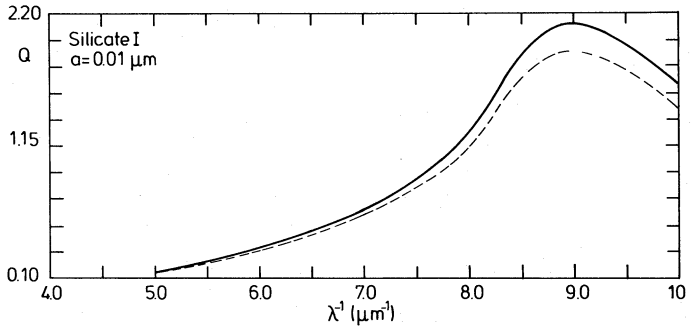

FIG. 9*c*

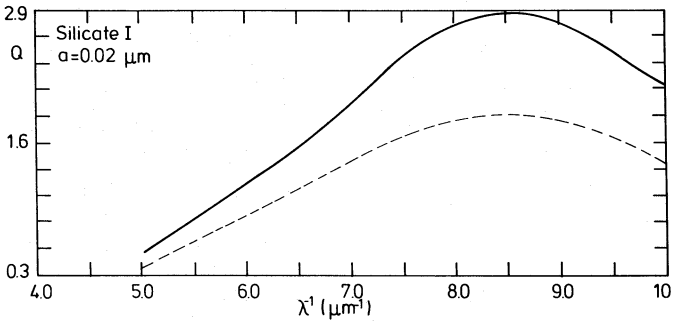

FIG. 9*d*

FIG. 9.—(*a*) Extinction cross sections of spherical silicate particles compared with the observed FUV extinction curve. The normalization is between $\lambda_1 = 1700$ Å (5.88 μm^{-1}) and $\lambda_2 = 1300$ Å (7.7 μm^{-1}). The values of the index of refraction used in the calculations are those of Huffman and Stapp (1971). (*b*)–(*d*) Extinction (*solid*) and absorption (*dashed*) efficiencies for silicate spheres of various radii. Index of refraction according to Huffman and Stapp (1971). Note the rapidly increasing scattering (extinction − absorption) for larger sizes.

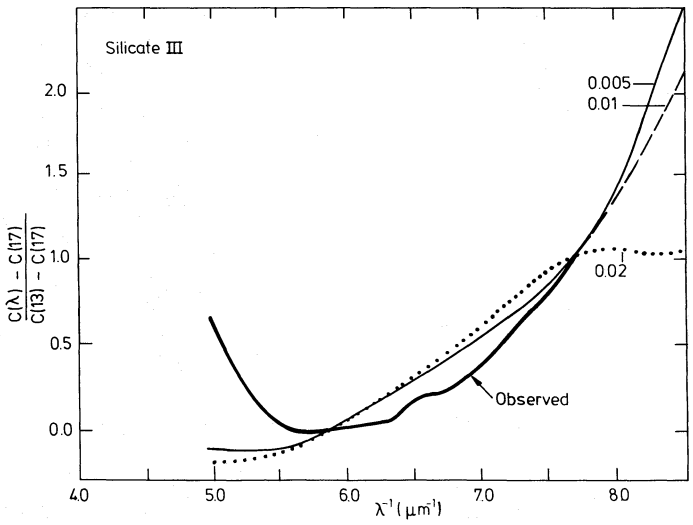

FIG. 10*a*

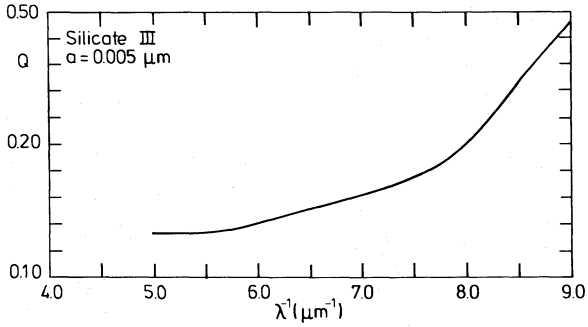

FIG. 10*b*

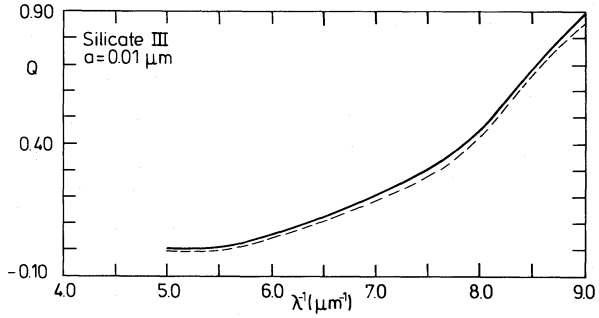

FIG. 10*c*

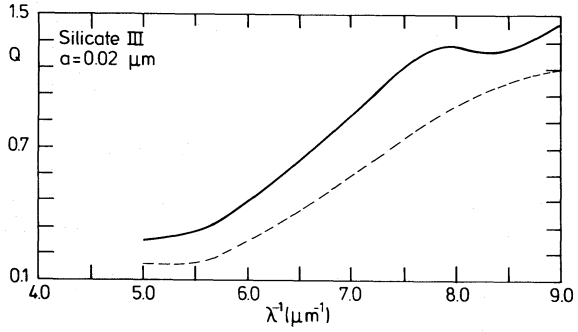

FIG. 10*d*

FIG. 10.—(*a*) Extinction cross sections for silicate spheres with hypothetical refractive indices (see text) compared with observations. The normalization is the same as in Fig. 9*a*. (*b*)–(*d*) Extinction (*solid*) and absorption (*dashed*) efficiencies for silicate spheres with indices of refraction the same as in Fig. 10*a*. Extinction − absorption = scattering.

absorption; i.e. *no scattering*. This condition is automatically satisfied by spheres in the Rayleigh approximation ($x \ll 1$) where the extinction is given by the absorption alone:

$$C_{\rm ext} \approx C_{\rm abs} = 9kV \frac{\varepsilon_2}{(\varepsilon_1+2)^2+\varepsilon_2^2} \sim \varepsilon_2 \lambda^{-1}, \qquad (1)$$

where $k = 2\pi/\lambda$, $V = 4/3\ \pi a^3$, $\varepsilon_1 = m'^2 - m''^2$, $\varepsilon_2 = 2m'm''$ and the complex index of refraction is $m(\lambda) = m'(\lambda) - im''(\lambda)$. In practice $x \leq 0.3$ is an adequate limit for validity of equation (1) (see van de Hulst 1957).

Although deviations from sphericity as well as variations in size produce differing extinctions, in the Rayleigh size limit the changes caused by nonsphericity are minor except where the particles have strong absorption bands (Greenberg 1972) which are clearly not present in interstellar materials between 1700 Å and 1300 Å.

Even allowing as much as 10% variability from uniform curvature limits the relative proportion of particle scattering to extinction to less than 10% over the full wavelength range up to $\lambda^{-1} = 7.7\ \mu{\rm m}^{-1}$. An examination of the calculated extinctions and absorptions for silicate particles in Figures 9 and 10 shows that they are restricted in size to $a \leq 0.01\ \mu$m. Scattering by graphite particles depends on their size in a similar way and leads to approximately the same restriction. Graphite particles as small as 0.01 μm make only an insignificant contribution to the FUV extinction (Fig. 8), whereas those whose size is such that they *would* contribute significantly at $\lambda^{-1} = 7.7\ \mu{\rm m}^{-1}$ are prohibited by the small scattering limitation.

We are thus led, on very general grounds, to the conclusion that the particles which may produce the 2160 Å hump (if they act at all like graphite particles) can not contribute to the FUV rise in extinction, and that the particles which produce the latter make a very small contribution at wavelengths longward of about 1700 Å or more correctly where they begin to absorb. These results provide the observational basis needed for the conjectured separation between the components labeled (3) and (4) in Figure 1.

To a certain extent what we have demonstrated from the theoretical scattering calculations can also be seen directly from the observations. Figures 3, 4, and 7 and Table 1 show that for exactly the same hump size the strength of the extra FUV component can vary by as much as a factor of about 3. Thus while the 2160 Å hump is well correlated with the visual extinction it varies independently of the FUV. It would be difficult to imagine even without the arguments based on particle scattering properties, that the hump and the FUV are not almost entirely due to separate species.

An immediate consequence of this result is that any model of interstellar grains for which the FUV extinction is produced by a sum of graphite and silicate contributions must be rejected. One recent example of this is the graphite plus silicate model proposed by Mathis, Rumpl, and Nordsieck (1977, hereafter MRN), for the average extinction curves. This violates both the nonscattering restriction and the component separation condition. The graphite particles in this model which produce the hump have a mean size well above 0.01 μm, and consequently they give rise to a major portion of the extinction at 1300 Å partly as a result of scattering. As stated in MRN, the extinction at λ2160 is "quite well distributed among the various sizes with roughly half contributed by particles [graphite] with $a > 0.04\ \mu$m." For particles as large as $a > 0.04\ \mu$m and even for smaller ones (see Fig. 8), the extra contribution to the FUV extinction is about the same (or larger) than the contribution to the hump, and they account for the FUV extinction. If we consider a variation of the FUV for a given hump size to be, say, a factor of one-half, the number of larger graphite particles must be reduced by this factor, and the number of small graphite particles must be accordingly increased enough to maintain the hump height. However, according to MRN (and see Fig. 8), the shape of the 2160 Å hump is strongly dependent on the size distribution. Consequently, variation in the relative strength of the hump to FUV would be accompanied by shifts in the position as well as the shape of the 2160 Å hump. However, this is not observed. The λ2160 band peak position appears rather to be quite insensitive to variations in the hump to FUV strengths. Thus, in order to preserve the 2160 Å hump shape while allowing for variations in the FUV, we are led to consider relative changes in the total *number* of graphite particles with respect to the number of silicate particles. We may examine the consequences of this procedure directly from Figure 4 of MRN. Subtracting the graphite extinction curve from the total extinction curve, we find that the silicate contribution to the FUV ($\lambda^{-1} \gtrsim 6\ \mu{\rm m}^{-1}$) is characteristic of relatively large particles and is curved downward even though in this distribution the silicate particles have a mean size too small to provide the proper polarization in the visual. Reducing the hump by the maximum observed factor of one-half relative to the average while maintaining the strength of the FUV extinction produces the extinction curve shown in column (3) of Table 2 where we have assumed the size distribution of the graphite and silicate components to be unchanged. We see that the deviations are *systematically* positive and that the maximum difference from the average is 0.34 which is 5 times the observed S.D. = 0.07 and is therefore unacceptable. The only way to compensate for this (while maintaining the shape of the 2160 Å hump) would be in the direction of *reducing* the relative number of large silicate particles, but this would distort the polarization curve even worse than already occurs in this model and is also inconsistent with the fact that our sample is supposed to be uniform in the

visual. As a second example we consider the value of $E(22-25)$ to be constant but allow $E(13-17)$ to be the minimum in our sample; namely, $E(13-17)/E(22-25) = 0.55$ times the average. This results in the values shown in column (4) of Table 2. Now, as expected, there is too great a contribution to the FUV shape by the graphite particles, thus producing an increase in the upward curvature of the FUV extinction. The deviations are now systematically negative relative to the average, and the maximum deviation is 8 times the standard deviation. In general, we deduce that using the basic MRN model, the observed variations in the FUV extinction can *only* be produced by accompanying variations in the visual polarization and extinction. It is important to recall that the variations we are referring to in this paper are in the diffuse cloud medium and are limited to the ultraviolet portion of the extinction curve. This means that these variations occur while maintaining a "standard" visual extinction curve. However, this does not mean that the existence of uniform FUV extinction curvature may not also extend into regions other than the diffuse medium.

We should emphasize that even though we have applied our criteria to a specific numerical grain model to show its level of compatibility with observations, the same inferences were already deduced on quite general grounds.

Another example of a model which fails to satisfy the proper conditions in the ultraviolet is that of Hong and Greenberg (1980). However, in this model the grains responsible for the visual extinction are independent of the grains (graphite plus silicate) which add the extra extinction in the ultraviolet so that there is not as strong a coupling between variations in the visual and ultraviolet extinction as in the MRN model composed solely of graphite plus silicate particles.

Finally, a rather significant consequence of the particle scattering criterion is that from the onset of the hump at about 4 μm^{-1} to at least 7.7 μm^{-1} the albedo of the small particles is essentially zero. The mean albedo in this short wavelength region is given by a weighted average including the contribution by the particles which produce the visual extinction. Particles whose size is ~ 0.1 μm^{-1} should have an albedo in the ultraviolet of about 1/2 (Greenberg 1978; van de Hulst 1957), so that the net albedo in the UV is given by

$$\alpha(\lambda^{-1}) \approx \frac{(Q_\infty/Q_V)A(V)\times 1/2 + \Delta A(\lambda^{-1})\times 0}{(Q_\infty/Q_V)A(V) + \Delta A(\lambda^{-1})}, \quad (2)$$

where $A(V)$ is the visual extinction, Q_V is the mean particle extinction efficiency at V, Q_∞ is the saturation extinction efficiency which we assume to be approached at $\lambda^{-1} \geq 4$ μm^{-1}, and $\Delta A(\lambda^{-1}) = A(\lambda^{-1}) - (Q_\infty/Q_V)A(V)$ is the extra extinction above the saturation extinction produced by the "visual" particles. The mean extinction efficiency of the "visual" particles at V is about 1.5 (Greenberg 1974) and at saturation is about 2 (van de Hulst 1957). For example, if $\Delta A(7.5)/A(V) = 0.5$ (a reasonable mean), the albedo at 7.5 μm^{-1} is about 0.37. In general, the ultraviolet albedos predicted in this way are smaller than those derived from measures of the diffuse galactic light (Witt and Lillie 1973) or from reflection nebulae (Witt 1977). Note that we make no predictions with regard to dense clouds where the number of small particles relative to the larger "visual" ones may be different and could be accountably smaller (Greenberg 1982) than in the diffuse cloud medium. For example, in Orion we predict an albedo of about 0.5 in the FUV because the FUV extinction is rather flat. This is confirmed by observations (Mathis *et al.* 1981). With regard to the scattering asymmetry factor in the ultraviolet, we need consider only the "visual" particles because the small particles scatter very little. Thus we expect that the value of $g = \langle \cos\theta \rangle$ would be approximately $g = 1$ throughout the ultraviolet regardless of the amount of extra FUV extinction. This results in a generally greater penetration of ultraviolet into clouds because of the reduction of the effect of multiple scattering.

TABLE 2

DEVIATIONS FROM THE AVERAGE FUV EXTINCTION PRODUCED BY VARIATIONS IN THE RELATIVE STRENGTHS OF THE FUV AND 2160 Å HUMP EXTINCTION ACCORDING TO A BIMODAL GRAPHITE PLUS SILICATE GRAIN MODEL[a]

λ^{-1} (μm^{-1}) (1)	$\frac{E(\lambda-17)}{E(13-17)}$ Average (2)	$0.5\times E(22-25)$ (3)	$0.55\times E(13-17)$ (4)
5.90	0.0	0.0	0.0
6.25	0.085	0.31	−0.30
6.80	0.31	0.65	−0.24
7.30	0.69	0.89	0.37
7.70	1.0	1.0	1.0

[a]Mathis *et al.* 1977.

b) *Implications on Grain Evolution*

A problem which requires a brief recapitulation here is the location of our program stars with respect to molecular clouds. As was stated in the § I, our study had to rely on very early-type stars because only these are bright enough to be observed in the ultraviolet at large distances. We know that such stars are almost always members of young clusters and are, as a rule, associated with molecular clouds. In order to limit ourselves to the D.C.M. (diffuse cloud medium), we had to introduce a limit criterion on the amount of molecular cloud "contamination." This we did by demanding that only

those stars could be accepted for which the difference between their $E(B-V)$ and the lowest $E(B-V)$ in the cluster, $[E(B-V)]_{\min}$, was substantially smaller than the value of $[E(B-V)]_{\min}$ itself. We also demanded that $[E(B-V)]_{\min}$ for each group be consistent with the amount of diffuse medium reddening implied by the distance to the cluster. In some cases, observations in different spectral regions (from radio to UV) indicate that the group of stars we are studying has already dispersed (or is still dispersing) the molecular material originally surrounding it so that the group is on the verge of emerging totally from its parent cloud. For example, see Lada *et al.* (1978) for consideration of IC 1805 which includes some of the O stars in our sample.

A further indication of the dominance of D.C.M. effects in our sample is that we have none of the anomalies which are commonly noted to appear in the 2200 Å hump feature or in the visual diffuse bands in dense clouds like those in Orion or Ophiuchus.

Although the evidence supports our contention that molecular cloud material makes a very limited contribution in our extinction samples, it is also obvious that at least some of the line-of-sight dust is being observed in the transition from the molecular cloud to the diffuse cloud phase. The fact that in our sample we achieve the same separation between the FUV extinction and the 2200 Å hump as did Massa (1980) who worked with spectra of B dwarfs, which are not likely to be affected by nearby molecular clouds, indicates that certain basic physical characteristics of the grain population responsible for the FUV extinction remain fairly stable once the grains have emerged from the molecular cloud phase of their evolution.

The high correlation between the visual extinction and the 2200 Å in the D.C.M. indicates that over the time scale in which these grains are outside molecular clouds there is an invariance in their relative contribution to the interstellar extinction. Since the cross sections for the particles providing the visual extinction ($2\pi a/\lambda \gtrsim 1$) are proportional to their area and the cross sections of the hump particles ($2\pi a/\lambda \ll 1$) are proportional to their volume (all absorption, no scattering), we may express this relative invariance as

$$\frac{N_V \bar{a}_V^2}{N_h \bar{a}_h^3} = \text{const}, \tag{3}$$

where $N_V, N_h, \bar{a}_V, \bar{a}_h$ are the column densities and the mean sizes of the "visual" and the "hump" particles, respectively. If we make the plausible assumption that both types of grains are equally coupled to the gas in the D.C.M., their relative number densities remain constant; i.e., $N_V/N_h = \text{const}$. It appears that if any change in the grains occurs it must be as a result of erosion, since growth in the D.C.M. is highly unlikely (Draine and Salpeter 1979*a b*, hereafter DSa, DSb; Greenberg 1982).

In terms of the mean volume erosion rate, τ_e^{-1}, defined in DSb, the particle radii decrease in time according to

$$a(t) = a_0 e^{-t/3\tau_e}, \tag{4}$$

where a_0 is the radius at time zero when the particle emerges from the molecular cloud.

Thus after a time τ in the D.C.M. equation (3) becomes

$$e^{-2\tau/3\tau_e^V}/e^{-3\tau/3\tau_e^h} = 1, \tag{5}$$

where $(\tau_e^V)^{-1}$ and $(\tau_e^h)^{-1}$ are the respective erosion rates for the "visual" and "hump" particles. In order to satisfy equation (5) these erosion rates must be in the proportion

$$(\tau_e^h)^{-1} = \tfrac{2}{3}(\tau_e^V)^{-1}. \tag{6}$$

The result given in equation (6) is quite general and is not dependent on the specific grain model. If we assume that the "visual" particles are core-mantle particles with organic refractory mantles and if the mantle material has an erosion rate in the D.C.M. which balances its growth rate in molecular clouds (Greenberg 1982), then it turns out that the inferred erosion rate for the "hump" particles is about the same as that of the 0.01 μm silicates as calculated in DSb. This is perhaps a not unrealistic result if the "hump" particles are graphite-like. However, by applying arguments similar to the above to the noncorrelation of the hump strength and the FUV extinction, we find lower erosion rates for graphite than for silicate particles (if the latter are assumed for the FUV). This means that the FUV particles are less resistant to sputtering than the 0.01 μm silicates of DSb. This is as far as we would like to hint here. A more detailed treatment of the consequences of the correlations and non correlations between the various extinction components on the evolutionary tracks of the various possible grain components is deferred to a later paper.

VI. SUMMARY

Comparing the values of the color excesses and the shapes of the extinction in the visual, the 2200 Å hump region, and the FUV region ($\lambda^{-1} \gtrsim 6$ μm^{-1}) for a sample of stars limited to the diffuse cloud medium we find that:

1. All far ultraviolet extinction curves follow the same functional form.

2. There is a substantial variation by as much as a factor of 3 in the relative strength of the hump and the FUV extinction.

3. The correlation between the strength of the 2200 Å hump and the visual extinction is confirmed.

From these findings, we have deduced the following consequences:

4. The particles responsible for both the 2200 Å hump and the FUV extinction have to be almost totally absorbing (little or no scattering) up to $\lambda^{-1} \approx 8\ \mu\mathrm{m}^{-1}$ and are therefore limited to sizes $\lesssim 0.01\ \mu$m.

5. The particles responsible for the 2200 Å hump and the FUV extinction constitute two independent populations, and the MRN graphite plus silicate model violates this condition.

6. The ultraviolet extinction by the particles responsible for the visual extinction is gray and therefore these particles constitute an entirely separate population from the hump particles or the FUV particles. Thus the full extinction curve is produced by a trimodal distribution of particles.

7. Although no "known" graphite or silicate particles which are limited in size by the "no scattering" criterion can produce the observed hump and FUV extinction, we can not exclude particles of related (but not yet well defined) chemical compositions being suitable candidates.

8. The correlation between the hump and visual extinction is accounted for if the respective particles have relative erosion rates in the diffuse cloud medium in the ratio 2:3 where this ratio is determined more by the particle size ratio than the material composition.

9. From the kinds of uniformity and even the kinds of variability in the interstellar extinction in the diffuse cloud medium we are led to a set of standards (a "benchmark") for the properties of the various grain populations with respect to which variations produced in other kinds of regions may be referred.

We would like to thank Dr. J. Krełowski and Dr. A. Strobel for selecting the original list of stars for use in our research. We thank Dr. H. C. van de Hulst for some useful suggestions.

APPENDIX

The extinction by a distribution of particles characterized by m shape and size parameters $a_1,\ldots,a_m$, is

$$A(\lambda) = \int_0^\infty \cdots \int_0^\infty n(a_1,\cdots,a_m) C(a_1,\cdots,a_m,\lambda)\, da_1 \cdots da_m, \tag{A1}$$

where $C(a_1,\cdots,a_m,\lambda)$ is the extinction cross section of an individual particle and $n(a_1,\cdots,a_m)$ is the particle distribution function. For simplicity we lump all size parameters into one so that equation (A1) is symbolically written as

$$A(\lambda) = \int_0^\infty n(a) C(a,\lambda)\, da. \tag{A1'}$$

For another distribution of particles $n'(a)$ the extinction is similarly

$$A'(\lambda) = \int_0^\infty n'(a) C(a,\lambda)\, da. \tag{A2}$$

Using the observed uniformity of curvature (uniform functional form) independent of the magnitude of the extinction in the far-ultraviolet, we can state that for any distribution function $n'(a)$ there exists a constant K such that $A'(\lambda) = KA(\lambda)$ or

$$\int_0^\infty n'(a) C(a,\lambda)\, da = K \int_0^\infty n(a) C(a,\lambda)\, da. \tag{A3}$$

A constant, K, satisfying equation (A3) exists if the extinction cross section separates into

$$C(a,\lambda) = F(a) \times G(\lambda). \tag{A4}$$

This is obviously a sufficient condition. It is also necessary. Let us assume that equation (A4) is not satisfied for all a and λ, so that we can find two wavelengths λ_1 and λ_2 such that

$$f(a) = \frac{C(a,\lambda_2)}{C(a,\lambda_1)}$$

is *not* independent of a. If we now choose $n'(a) = f(a) \times n(a)$, it is easy to show that the "constant" K_1 which satisfies

equation (A3) for $\lambda = \lambda_1$ is different from the "constant" K_2 which satisfies equation (A3) for $\lambda = \lambda_2$. This, however, contradicts the existence of a single constant K for all wavelengths. Therefore $C(a, \lambda) = F(a)G(\lambda)$ is both a necessary and sufficient condition for the uniform FUV extinction.

REFERENCES

Bless, R. C., and Savage, B. D. 1970, in *IAU Symposium 36, Ultraviolet Stellar Spectra and Related Ground-Based Observations*, ed. L. Houziaux and H. E. Butler (Dordrecht: Reidel), p. 28.
_____. 1972, *Ap. J.*, **171**, 293.
Bohlin, R. C., Holm, A. V., Savage, B. D., Snijders, M. A. J., and Sparks, W. M. 1980, *Astr. Ap.*, **85**, 1.
Boggess, A., and Borgman, J. 1964, *Ap. J.*, **140**, 1636.
Boggess, A., *et al.* 1978*a*, *Nature*, **275**, 372.
Boggess, A., *et al.* 1978*b*, *Nature*, **275**, 377.
Dorschner, J., Friedeman, C., and Gürtler, J., 1977, *Astr. Ap.*, **58**, 201.
Draine, B. T., and Salpeter, E. E., 1979*a*, *Ap. J.*, **231**, 77 (DSa).
_____. 1979*b*, *Ap. J.*, **231**, 438 (DSb).
Duley, W. W. 1976, *Ap. Space Sci.*, **45**, 253.
Duley, W. W., and Millar, T. J. 1979, *Ap. J.* (*Letters*), **233**, L87.
Duley, W. W., Millar, T. J., and Williams, D. A. 1979, *Ap. Space Sci.*, **65**, 69.
Egan, W. G., and Hilgeman, T. 1974, *Bull. AAS*, **6**, 433 (EH).
_____. 1975, *A.J.*, **80**, 587 (EH).
Greenberg, J. M. 1972, *J. Colloid Interface Sci.*, **39**, 513.
_____. 1973, in *IAU Symposium 52, Interstellar Dust and Related Topics*, ed. J. M. Greenberg and H. C. van de Hulst (Dordrecht: Reidel), p. 3.
_____. 1974, *Ap. J.* (*Letters*), **188**, L81.
_____. 1978, in *Cosmic Dust*, ed. J. A. M. McDonnell (New York: J. Wiley and Sons), p. 187.
_____. 1982, in *Submillimetre Wave Astronomy*, ed. J. P. Phillips and J. Beckman (Cambridge: Cambridge University Press), p. 261.
Greenberg, J. M. and Hong, S. S. 1974, in *Proc. 8th ESLAB Symposium on* H II *Regions and the Galactic Centre*, ed. A. F. M. Moorwood (ESRO SP-105), p. 153.
Greenberg, J. M. and Shah, G. A. 1969, *Physica*, **41**, 92.
Henize, K. G., Wray, J. D., and Parsons, S. B. 1982, *A.J.*, **86**, 1658.
Holm, A. V., and Cassinelli, J. P. 1977, *Ap. J.*, **211**, 432.
Hong, S. S., and Greenberg, J. M. 1980, *Astr. Ap.*, **88**, 189.
Huffman, D. R, Stapp, J. L. 1971, *Nature Phys. Sci.*, **228**, 45 (HS).
Jamar, C. Macau-Hercot, D., Monfils, A., Thompson, G. I., Houziaux, L., and Wilson, R. 1976, *Ultraviolet Bright-Star Spectrophotometric Catalogue*, (Paris: European Space Agency).
Lada, C. J., Elmegreen, B. G., Cong, H. J., and Thaddeus, P. 1978, *Ap. J.* (*Letters*), **226**, L39.
Macau-Hercot, D., Jamar, C., Monfils, A., Thompson, G. I., Houziaux, L., and Wilson, R. 1978, *Supplement to the Ultraviolet Bright-Star Spectrophotometric Catalogue* (Paris: European Space Agency).
MacLean, S., Duley, W. W., Millar, T. J. 1982, *Ap. J.* (*Letters*), **256**, L61.
Massa, D. 1980, *A.J.*, **85**, 1651.
Mathis, J. S., Perinotto, M., Patriarchi, P., and Schiffer, F. H., III, 1981, *Ap. J.*, **249**, 99.
Mathis, J. S., Rumpl, W., and Nordsieck, K. H. 1977, *Ap. J.*, **217**, 425 (MRN).
Nandy, K., Thompson, G. I., Jamar, C., Monfils, A., and Wilson, R. 1975, *Astr. Ap.*, **44**, 195.
Savage, B. D. 1975, *Ap. J.*, **188**, 92.
Seaton, M. J. 1979, *M.N.R.A.S.*, **187**, 73P.
Sitko, M. L., Savage, B. D., and Meade, M. R. 1981, *Ap. J.*, **246**, 161.
Stecher, T. P. 1965, *Ap. J.*, **142**, 1683.
Taft, E. A. and Phillips, H. R. 1965, *Phys. Rev.*, **138**, A187.
Tosatti, B., and Bassani, F. 1970, *Nuovo Cimento*, **65B**, 161.
van de Hulst, H. J. 1957, *Light Scattering by Small Particles* (New York: J. Wiley and Sons).
Walborn, N. 1982, *Ap. J.* (*Letters*), **254**, L15.
Whittet, D. C. B., and van Breda, I. G. 1975, *Ap. Space Sci.*, **38**, L3.
Whittet, D. C. B., van Breda, I. G., and Glass, I. S. 1976, *M.N.R.A.S.*, **177**, 625.
Witt, A. N. 1977, *Pub. A.S.P.*, **89**, 750.
Witt, A. N., and Lillie, C. F. 1973, *Astr. Ap.*, **25**, 397.
Wu, C. C., York, D. G., and Snow, T. P. 1981, *A.J.*, **86**, 755.

GRZEGORZ CHLEWICKI and J. MAYO GREENBERG: Laboratory Astrophysics, University of Leiden, P.O. Box 9504, Wassenaarseweg 78, 2300 RA Leiden, The Netherlands